University of Groningen

Superparamagnetic iron oxide nanoparticles alter expression of obesity and T2D-associated risk genes in human adipocytes

Sharifi, S.; Daghighi, S.; Motazacker, M. M.; Badlou, B.; Sanjabi, B.; Akbarkhanzadeh, A.; Rowshani, A. T.; Laurent, S.; Peppelenbosch, M. P.; Rezaee, Farhad

IMPORTANT NOTE: You are advised to consult the publisher's version (publisher's PDF) if you wish to cite from it. Please check the document version below.

Document Version
Publisher's PDF, also known as Version of record

Publication date:
2013

Link to publication in University of Groningen/UMCG research database

Citation for published version (APA):
Sharifi, S., Daghighi, S., Motazacker, M. M., Badlou, B., Sanjabi, B., Akbarkhanzadeh, A., ... Rezaee, F. (2013). Superparamagnetic iron oxide nanoparticles alter expression of obesity and T2D-associated risk genes in human adipocytes. Scientific Reports, 3, [2173]. DOI: 10.1038/srep02173

SCIENTIFIC REPORTS

Superparamagnetic iron oxide nanoparticles alter expression of obesity and T2D-associated risk genes in human adipocytes

S. Sharifi[1]*, S. Daghighi[1]*, M. M. Motazacker[2], B. Badlou[3], B. Sanjabi[4], A. Akbarkhanzadeh[5], A. T. Rowshani[6], S. Laurent[7], M. P. Peppelenbosch[8] & F. Rezaee[8,9]

[1]Department of Biomedical Engineering, W.J. Kolff Institute, University Medical Center Groningen and University of Groningen, Groningen, The Netherlands, [2]Department of Vascular Medicine, Academic Medical Center, University of Amsterdam, Amsterdam, The Netherlands, [3]BB Research institute, Utrecht, The Netherlands, [4]University of Groningen, University Medical Center Groningen, Department of genetics, Groningen, The Netherlands, [5]Bioscience, Free University of Amsterdam, Amsterdam, The Netherlands, [6]Department of transplantation, Erasmus Medical Center, Rotterdam, The Netherlands, [7]Department of General, Organic, and Biomedical Chemistry, NMR and Molecular Imaging Laboratory, University of Mons, Mons, Belgium, [8]Department of Gastroenterology and Hepatology, Erasmus Medical Center, Rotterdam, The Netherlands, [9]University of Groningen, University Medical Center Groningen, Dept. Cell Biology, Groningen, The Netherlands.

Adipocytes hypertrophy is the main cause of obesity and its affliction such as type 2 diabetes (T2D). Since superparamagnetic iron oxide nanoparticles (SPIONs) are used for a wide range of biomedical/medical applications, we aimed to study the effect of SPIONs on 22 and 29 risk genes (Based on gene wide association studies) for obesity and T2D in human adipocytes. The mRNA expression of lipid and glucose metabolism genes was changed upon the treatment of human primary adipocytes with SPIONs. mRNA of GULP1, SLC30A8, NEGR1, SEC16B, MTCH2, MAF, MC4R, and TMEM195 were severely induced, whereas INSIG2, NAMPT, MTMR9, PFKP, KCTD15, LPL and GNPDA2 were down-regulated upon SPIONs stimulation. Since SEC16B gene assist the phagocytosis of apoptotic cells and this gene were highly expressed upon SPIONs treatment in adipocytes, it is logic to assume that SPIONs may play a crucial role in this direction, which requires more consideration in the future.

A dipocytes hypertrophy is the major cause of obesity, which promotes an inflammation state and this, in turn, is implicated with pathophysiological metabolic disorders[1,2] such as insulin resistance (IR), type 2 diabetes (T2D) and cardiovascular disease (CVD)[3–6]. While adipocytes play a central role in maintaining lipid homeostasis and energy balance, recent studies suggest that adipose tissue (AT) is a key site for chronic inflammation in obese human subjects and rodents[7,8], and the macrophage content of AT in obese humans and rodents increases dramatically. Meijer *et al.*[2] has recently shown that adipocytes exhibit immune cell function and are able to prime inflammation independent of macrophages. For example, hypertrophic adipocytes in obese individuals alter the adipose tissue macrophages (ATMs) from resident to activated macrophages, secreting secrete a range of cytokines and chemokines, which the latter recruit T cells towards AT. Since obesity and its associated metabolic disorders are multifactorial disease and adipocytes hypertrophy is the main cause of obesity, a comprehensive approach to identify biological and functional pathways of adipocytes-genes associated with the diseases is necessary to clarify the molecular signatures of obesity and related diseases[9–11]. Based on epidemiological and gene wide association studies (GWAS), one cluster of genes is considered as potential risk for obesity and one gene cluster is potentially involved in the development of T2D[12]. In fact gene expression can be influenced by many factors including organism's internal signals as well as external environment factors[13].

With the rapid advances of nanoscience and nanotechnology, our exposure to nanomaterials is significantly increasing, however, the potential risks of these nanomaterials are largely unknown[14,15]. Because of their very small size, nanoparticles (NPs) are capable of entering the human body by inhalation, ingestion, skin penetration or via injections; in this case, it may be assumed that NPs have capability to interact with intracellular structures

and macromolecules for long periods[16,17]. One particularly important toxicological endpoint is genotoxicity, as large-scale gene expression analysis provides a logical approach to study the detailed mechanisms of NPs toxicity. Recent studies have shown that NPs can changes gene expression, thus, altering cellular functions or even NPs could be the cause of toxicity[18–20].

The aim of this study is to investigate whether superparamagnetic iron oxide nanoparticles (SPIONs) affect down or up-regulation of two cluster genes involved in the development of obesity and T2D in human primary adipocytes. SPIONs are amongst the most used NPs in medicine and they have been investigated for many applications, including magnetic labeling[21,22], cell isolation[23], hyperthermia[24], and controlled drug release[25]. Due to their small size, these NPs can produce excess reactive oxygen species (ROS) through their dissolution and formation of $OOH^{\bullet}$ and $OH^{\bullet}$ radicals from H_2O_2 via the Fenton reaction[26–28]. Moreover, the obesity-induced oxidative stress and localized inflammation in AT leads to important changes in adipocyte gene expression with downstream effects on adipocyte lipid metabolism and triglycerides as the stored energy in the lipid droplets[29,30]. Since adipocytes hypertrophy is the main cause of obesity and, in turn, T2D, we design this study to investigate the effect of SPIONs on 22 and 29 risk genes associated with obesity and T2D in human primary adipocytes.

Results

Synthesis and characterization of SPIONS. The Fourier transform infrared spectroscopy (FTIR) generated spectra of bare SPIONs and Carboxyethylsilanetriol (CES) grafted SPIONs are shown in Figure 1. The broad band at 3400–3500 cm^{-1} indicated the presence of surface hydroxyl groups in bare SPIONs (Figure 1A). In the FTIR spectrum of CES-grafted SPIONs (see Figure 1B), a strong peak at 1709 cm^{-1} is present due to acidic carbonyl (C=O) groups. Symmetric and asymmetric stretching vibrations of methylene groups in CES showed absorption bands at 2931 and 2867 cm^{-1}, respectively. Strong peak at 1087 cm^{-1} is due to C–O of CES group. The absorption band at 1460 cm^{-1} is due to bending vibrations of CH_2 groups of CES groups.

TEM of the SPIONs is shown in Figure 2A and 2B confirming the formation of SPIONs with a very narrow size distribution. More quantitative analyses of particles were conducted using magnetometry and relaxometry. In Figure 2D and 2C, these corresponding

curves of the SPIONs are shown. A Langevin function was fitted to the data, providing a particle radius R of 4.73 and saturation magnetization (Ms) of 56.48 A m^2/kg for CES grafted SPIONs. Particle radius and saturation magnetization (Ms) of bare SPIONs were found to be 4.67 and 53.24 A m^2/kg respectively. The Nuclear Magnetic Relaxation Dispersion (NMRD)-profile of a SPIONs is reported on Figure 2B. As it is clear from the picture, R1 values increased after grafting with CSE. The curve represents a peak in the high field (10–60 MHz), which is due is slow rotational correlation time of self-agglomerates.

The effect of SPIONs on high risk genes associated with obesity and type 2 diabetes in human primary adipocytes. *The mRNA analysis of high risk genes-associated with obesity and type 2 diabetes.* The procedure for growth of human primary adipocytes was already described[2,7]. To investigate whether SPIONs affect the expression of high risk genes associated with obesity and T2D, mRNA expression of 22 and 29 genes with high susceptibility to obesity and T2D, respectively, were measured in human primary adipocytes, which were already established as an energy metabolism model. Upon SPIONs stimulation, most of these adipocyte-associated high-risk genes for obesity were down-regulated and a few up-regulated such as (*e.g.* INSIG2, NAMPT (also called Visfatin, which is mainly present in adipocytes), MTMR9, PFKP, KCTD15, LPL and GNPDA2 highly down-regulated) and (*e.g.* NEGR1, SEC16B, MTCH2, MAF and MC4R highly up-regulated)) as depicted in Figure 3. However, three genes DGKG, NCR3 and PTER were not detected in human primary adipocytes treated with and without SPION.

The mRNA expression of high-risk genes associated with T2D was also measured in human primary adipocytes, upon SPIONs treatment. As depicted in Figure 4, after stimulation of human primary adipocytes with SPIONs, the majority of high risk genes linked with T2D was highly down regulated such as PPAR-γ, IGF2BP2, WFS1, JAZF1, CAMK1D, PRC1, TCF7L2 and ZFAND6. The other genes such as GULP1, SLC30A8, and TMEM195 were severely induced upon SPIONs stimulation as compared to control. The mRNA of the following genes KCNJ11, HHEX, and HNF1B were not detectable in either state.

Functional pathway and disorder analysis of *obesity-associated genes* in human primary adipocytes upon SPION stimulation.
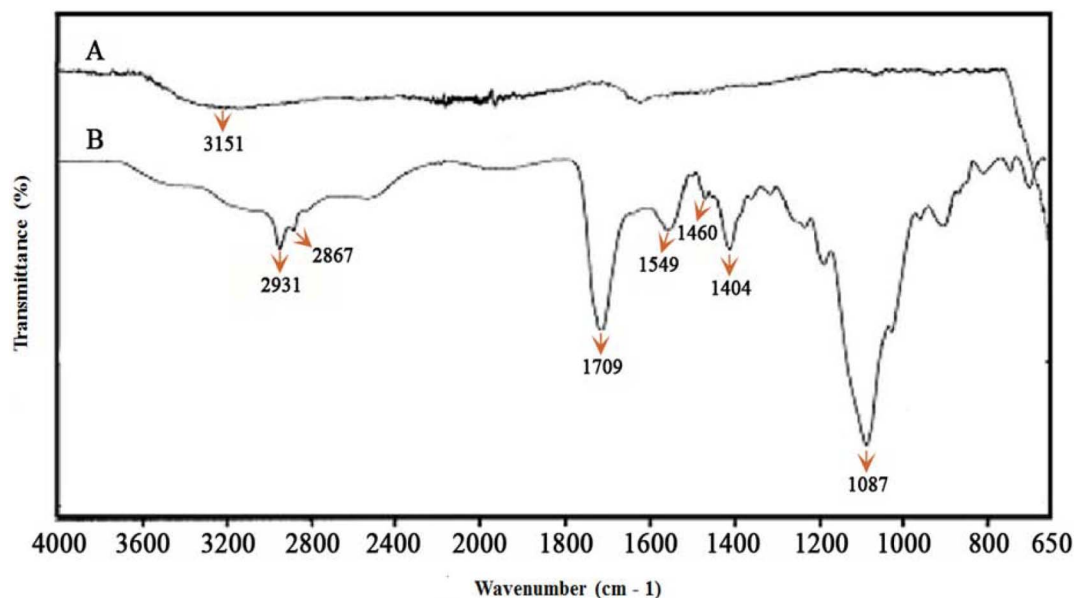

Figure 1 | Fourier Transform Infrared Spectroscopy (FTIR) of (A) bare and (B) CES-grafted SPIONs.
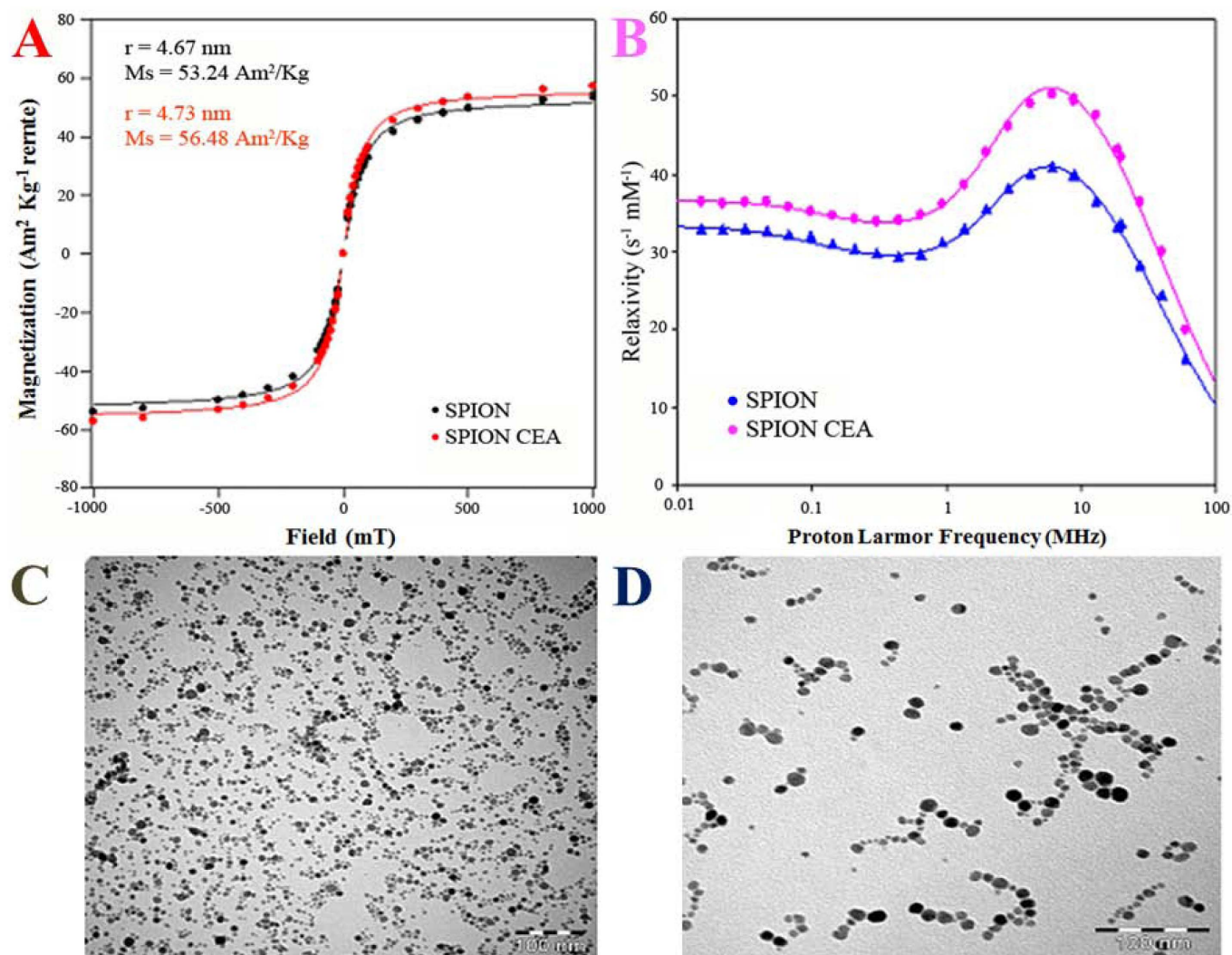
Figure 2 | Magnetization curves, NMRD profiles, and Transmission Electron Micrographs of bare and CES-grafted SPIONS. (A) Magnetization curves for bare and CES-grafted SPIONs, (B) NMRD profiles of bare and CES-grafted SPIONs, and Transmission Electron Micrographs of (C) bare and (D) CES-grafted SPIONs.

To gain more insight into the possible physiological functions of obesity-associated genes, statistically enriched pathways and diseases for the 22 genes involved in obesity were investigated using KOBAS 2.0. KOBAS 2.0 was combined with hypergeometric test and Benjamini-Hochberg FDR correction and considering all human genes as background. This included Kyoto Encyclopedia of Genes and Genomes (KEGG) pathway, Pathway Interaction Database (PID) curated, PID BioCarta, PID reactome, BioCyc, Reactome and Protein Analysis Through Evolutionary Relationships (PANTHER) pathway databases and KEGG disease, Genetic Association Database (GAD), Functional disease ontology (FunDO), Online Mendelian Inheritance in Man (OMIM) and National Human Genome Research Institute (NHGRI) human disease databases. Functional Pathways and disorders with a corrected p-value < 0.05 were considered relevant and are shown in Figure 5 and 6 respectively. 4 functional pathways were found to be related to Glycerolipid metabolism (KEGG), adipocytokine signaling pathway (KEGG), N-acetylglucosamine metabolism (PANTHER) and 2-arachidonoylglycerol biosynthesis (PANTHER). These data further illustrated that lipids and glucose also have a key role in these pathways. These four pathways were resulted from only 5/22 analyzed genes of which three genes were adipocytes differentiation markers (*e.g.* ADIPOR1, ADIPOR2, and LPL) (Figure 5). Upon

SPION treatment, all genes found in this pathway were down-regulated in adipocytes as compared to control adipocytes, except DGKG, which was not detectable in either state.

Subsequently, we investigated whether obesity-associated genes could have a role in human diseases. As displayed in Figure 6, 8 diseases were screened of which 5 appeared to be involved in lipid metabolism and AT. Importantly, one disorder related to hyperinsulinism, which may be also caused by an increase of AT-mass. Based on disorder enrichment analysis, obesity-associated genes involve in the development of human polycystic ovary syndrome. The disorder analysis also revealed that weight (*i.e.* 10 genes from 19 genes in this pathway) and body mass index (BMI) (*i.e.* 10 from 23 genes in this pathway) were considered as the most enriched disease processes, which fits well with the known involvement of these two factors in obesity disease, although it also suggests that the contribution of fat mass increase to hyperinsulinism might be due to the expression of insulin by AT and in particular adipocytes. It is noteworthy to mention that weight is one of two factors in BMI equation and obesity can be calculated by BMI. Importantly, disorder enrichment analysis showed that metabolic disorders (*i.e.* 20 from 719 genes present in this pathway) constituted approximately gene coverage of 3–4% as identified by disorder enrichment analysis. As depicted in Figure 6, the second hit of disorder analysis is BMI and covered by 10 genes of

Figure 3 | mRNA expression of 22 genes associated with obesity as found by GWAS was analyzed in adipocytes after treatment with and without SPIONs. mRNA expression of 22 genes was expressed as ^{2}log values on the y-axis. Relative mRNA intensity was obtained from two measurements.

which 5 genes (*i.e.* MCR4, TMEM18, MTCH2, NEGR1 and SEC16B) show a higher mRNA expression in SPION adipocytes than control adipocytes and 4 genes display an opposite version. DGKG was not detected in both states. Moreover, the sixth hit of disorder analysis is obesity with 5 genes of which after SPIONs treatment the expression of two genes (*i.e.* MAF and MC4R) go up and two genes (*i.e.* NAMPT and INSIG2B) goes down and one gene (*i.e.* PTER) not detected in both states.

Functional pathway and disorder analysis of *T2D-associated genes* in human primary adipocytes upon SPIONs stimulation. To shed more light into the possible physiological functions of T2D-associated genes, statistically enriched pathways and diseases for the 29 genes involved in T2D were detected using the same procedure and databases as we applied for obesity-associated genes. Functional Pathways and disorders with a corrected p-value < 0.05 were considered relevant and are shown in Figure 7 and 8
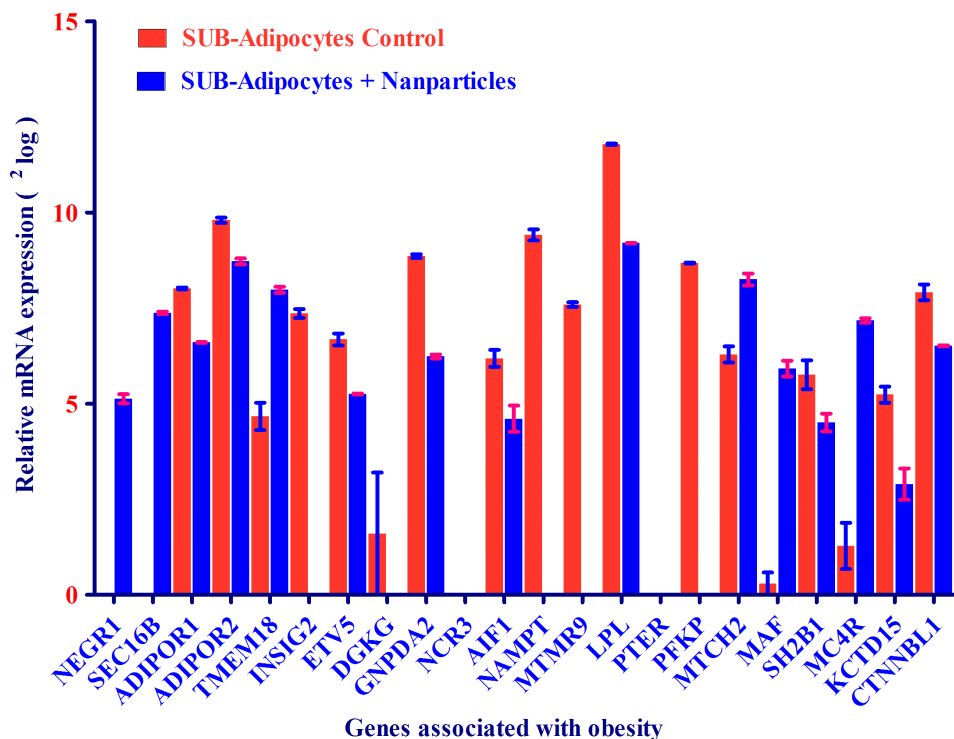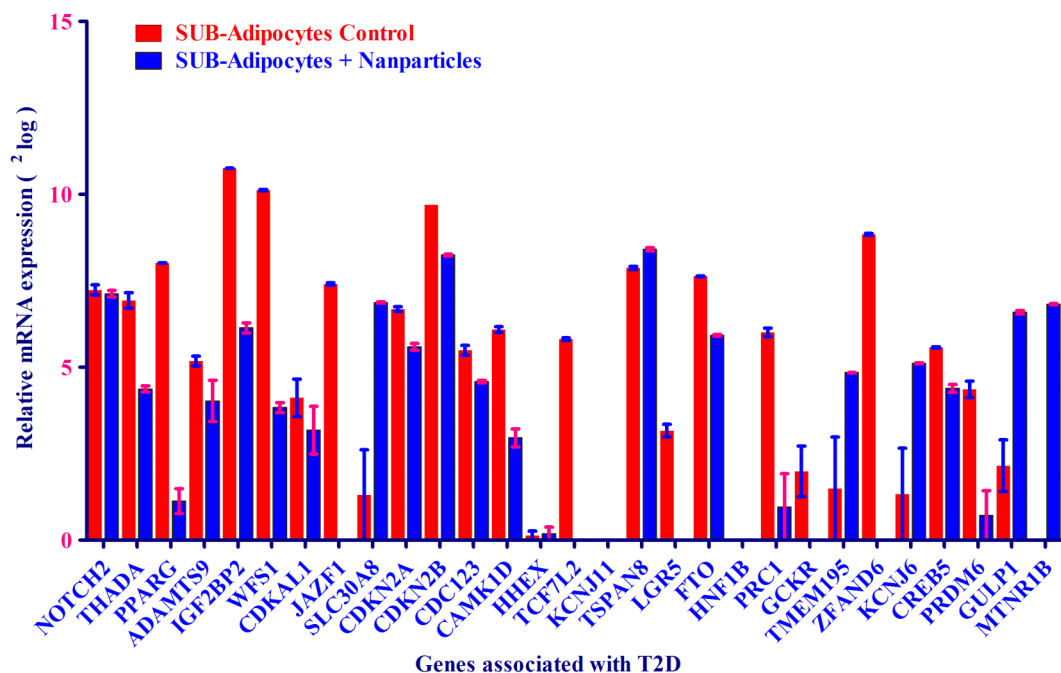

Figure 4 | mRNA expression of 29 genes associated with type 2 diabetes (T2D) as found by GWAS was analyzed in adipocytes after treatment with and without SPIONs. mRNA expression of 29 genes was expressed as ^{2}log values on the y-axis. Relative mRNA intensity was obtained from two measurements.
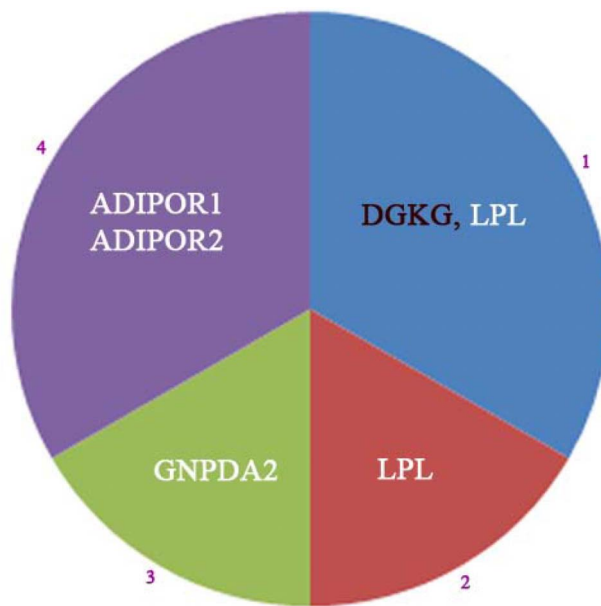
1. KEGG PATHWAY: Glycerolipid metabolism
2. PANTHER: 2-arachidonoylglycerol biosynthesis
3. PANTHER: N-acetylglucosamine metabolism
4. KEGG PATHWAY: Adipocytokine signaling pathway

Figure 5 | Enriched pathways related to the 22 genes found by Gene Wide Association Study (GWAS) as risk genes for obesity. The abbreviations or description is: Kyoto Encyclopedia of Genes and Genomes (KEGG), and Gene Analysis Through Evolutionary Relationships (PANTHER). Only pathways with corrected p-values < 0.05 are presented. Abbreviations in Figure are: ADIPOR1 and 2 (Adiponectin receptor gene 1 and 2), LPL (lipoprotein lipase), DGKG (Diacylglycerol kinase gamma), and Glucosamine-6-phosphate isomerase 2. The complete list of abbreviations was shown in table 1.

1. GAD: Weight
2. GAD: Body mass index
3. GAD: METABOLIC
4. FunDO: Hyperinsulinism
5. FunDO: Polycystic ovary syndrome
6. GAD: obesity

Figure 6 | Enriched disorder pathways related to the 22 genes found by GWAS as risk genes for obesity. The abbreviations or description is: Genetic Association Database (GAD), and Functional disease ontology (FunDO). Only disorders with corrected p-values < 0.05 were included in the analysis. The complete list of abbreviations was shown in table 1.

respectively. 4 functional pathways were found of which 2 played a role in the cell cycle and cell check point (*i.e.* PID BioCarta) as depicted in Figure 7. However, only one pathway was found to be directly related to diabetes (*i.e.* KEGG). The last detected functional pathway was Thyroid cancer (*i.e.* KEGG). These 4 functional pathways were found by PID BioCarta and KEGG databases and include 6/29 genes of which mRNA expression of 4 genes (*i.e.* PPARγ, TCF7L2, CDKN2A and CDKN2B) were down-regulated or not detected upon treatment of adipocytes with SPION and two genes (*i.e.* HHEX and HINF1B) were not detected in either state.

T2D-associated genes were also examined whether they could have a role for human diseases. As depicted in Figure 8, the majority of found disorders are T2D as expected. Also 4 disorders were identified of which two diseases related to the metabolism and two associated with glucose metabolism. These two disorders also considered to be truly involved in T2D. Another disorder was matched to the intracranial aneurysm, which may be due to T2D as cause of this disease. Disorder enrichment analysis logically revealed that (*i.e.* 15–24/29 genes) T2D, glucose metabolism in general were considered as the most enriched disease processes identified by disorder enrichment analysis, which matches well with the known role of these factors in T2D disease. Since all disorders ended to T2D, we have chosen to dissection the hit number 1 (Figure 8), which pointed to T2D includes 18 genes of 25 genes found in this pathway (*i.e.* GAD database; hit 1); a coverage of 70% (18 : 25 genes). Upon SPIONs treatment, importantly, mRNA expression of 11 genes (*i.e.* CDC123, CAMK1D, IGF2BP2, CDKN2A, JAZF1, FTO, LGR5, TCSF7-L2, PPARγ, CDKN2B, and THADA) was down-regulated as compared to control adipocytes. Two genes (*i.e.* KCNJ11 and HHEX) were neither detected in SPIONs adipocytes nor control. However, mRNA expression of four genes (*i.e.* ADAMTS9,

CDKAL1, NOTCH2 and TSPAN8) was equal for both states and one gene (*i.e.* SLC30A8) up-regulated in SPION adipocytes.

Functional pathway and disorder analysis of combined set genes associated with obesity and T2D in human primary adipocytes upon SPION stimulation. To obtain further insight into the specific roles that obesity- and T2D-associated genes might have in pathophysiology, we also analyzed the combined set of genes linked with these two disorders (see Table 1, Figure 9 and Figure 10).

KOBAS version 2.0 was also applied to detect the functional and disorder pathways in this combined set of genes. As exhibited in Figure 9, unexpectedly, we found only three pathways of which two pathways appeared to have a role in lipid metabolism and one pathway in cell cycle. PPARγ and LPL genes were accounted for lipid metabolism, and CDKN2A and CDKN2B are responsible for cell cycle[31–33]. Upon SPIONs treatment, mRNA expression of LPL and PPARγ severely down-regulated in adipocytes as compared to control adipocytes. Regarding CDKN2A and CDKN2B, as depicted in Figure 3 and 4 they are slightly down-regulated after treatment of adipocytes with SPIONs.

Based on disorder enrichment analysis, we detected 19 hits of which weight, BMI and T2D were considered as the most enriched disease process identified by disorder enrichment analysis, which fits well with the known involvement of these genes in the development of these two diseases as noted by Gene Wide Association study (*i.e.* GWAS). As depicted in Figure 10, The GAD and KEGG databases analysis (*i.e.* hit number 1 and 2 respectively) revealed that diabetes (*i.e.* 18 from 25 genes found in hit 1, and 16 from 19 genes detected in hit 2) and weight (*i.e.* 11 from 19 genes identified by GAD database analysis; hit number 4) as well as BMI (*i.e.* 11 from 23 genes screened in this database; hit number 5) are the most enriched disease pathways. T2D covered approximately 75–80% of this disease

1. PID BioCarta: cyclins and cell cycle regulation
2. PID BioCarta: cell cycle: g1/s check point
3. KEGG PATHWAY: Maturity onset diabetes of the young
4. KEGG PATHWAY: Thyroid cancer

Figure 7 | Enriched pathways related to the 29genes found by GWAS as risk genes for type 2 diabetes (T2D). The abbreviations or description is: Kyoto Encyclopedia of Genes and Genomes (KEGG), and gene Analysis through Evolutionary Relationships (PANTHER). Only pathways with corrected p-values < 0.05 are presented. Abbreviations are: CDKN2A and B (Cyclin-dependent kinase inhibitor 2A and B, isoform 4), PPARγ (Peroxisome proliferator-activated receptor gamma), HHEX (Hematopoietically expressed homeobox protein HHEX), TCF7L2 (Transcription factor 7-like 2) HNF1B (Hepatocyte nuclear factor 1). The complete list of abbreviations was shown in table 1.
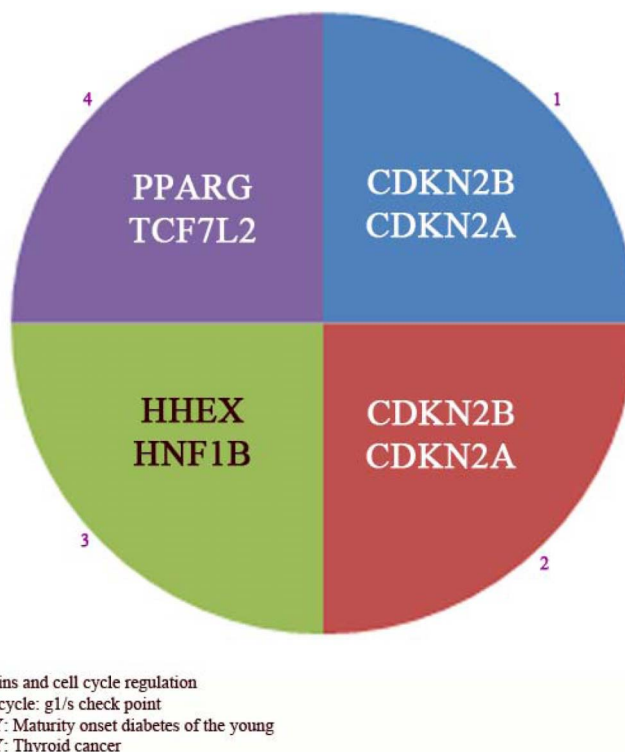
Figure 8 | Enriched disorder pathways linked to the 29 genes found by GWAS as risk genes for type 2 diabetes (T2D). The abbreviations are: Kyoto Encyclopedia of Genes and Genomes (KEGG), Genetic Association Database (GAD), and Functional disease ontology (FunDO). Only disorders with corrected p-values < 0.05 were included in the analysis. The complete list of gene abbreviations was shown in table 1.

pathway and weight/BMI showed pathway coverage of about 50%. The disorder analysis obesity-associated genes are also involved in the human polycystic ovary syndrome. Disorder T2D was identified by GAD database (*i.e.* hit number 1) includes 18 genes of which, upon SPIONs treatment, 7 genes like CDKAL1 were severely, 4 genes slightly such as CDKN2B down-regulated. However, the expression of 4 genes was remained unchanged like ADAMTS9 and two genes (*i.e.* HHEX and KCNJ11) were not detected, when we compare control adipocytes with SPION adipocytes. Notably, only 1 gene (*i.e.* SLC30A8) was highly expressed upon SPION treatment as compared to control (Figure 3 and Figure 10). Surprisingly, based on GAD database (hit 5) BMI disorder is the most prominent disease. In this regard, the mRNA expression of 5 genes (MC4R, TMEM18, MTCH2, SEC16B, and NEGR1) was highly up-regulated in SPIONs adipocytes comparing with control adipocytes. DGKG gene was not detected in either state. The rest of genes like FTO were expressed higher in control adipocytes than SPIONs adipocytes (see Table 1 and Figure 10, hit 5).

Differences and similarities between before and after treatment of human adipocytes with SPIONs with respect to mRNA expression. We found the expression of 6 genes from 22 genes-linked with obesity up-regulated after treatment with SPION as compared to control adipocytes. Notably, the mRNA expression of NEGR1,

SEC16B and MAF was not detectable and MCR4 was just detected as traces (Figure 3 and table 1), indicating that 30% of the obesity genes were up-regulated after treatment of the cells with SPIONs. Whereas, the mRNA of INSIG2, NAMPT, and MTMR9 were not detectable upon treatment of adipocytes with SPIONs as compared to control cells. In addition, three genes (*i.e.* DGKG, NCR3, and PTER) were not expressed in both states; upon SPION treatment and control. Finally, the rest of obesity-associated genes were shown to have a higher mRNA expression in control adipocytes than adipocytes after SPIONs treatment.

We observed an equal mRNA expression of NOTCH2, ADAMTS9, CDKAL1, TSPAN8 and PRDM6 (as a part of T2D-associated genes) for both control and SPION adipocytes. There was no mRNA expression observed for HHEX, HNF1B and KCNJ11 for either state. As depicted in Table 1 and Figure 4, mRNA expression of the following genes MTNR1B, GULP1, KCNJ6, CDKN2B, and TMEM195 were found to be higher in human adipocytes upon SPIONs treatment than control adipocytes. The remaining genes from T2D cluster genes showed a higher mRNA expression in control adipocytes than SPION adipocytes.

Discussion

An imbalance or dysfunction of adipocytes leads to obesity. Obesity is linked with metabolic disorders and in particular insulin resistance,

Table 1 | The analysis of Risk genes associated with obesity and type 2 diabetes in adipocytes after treatment with and without SPIONs

| Gene Name	Gene Description	Disease (GWAS)	MW (kDa)	pI	AD Exp	Adipocytes + SPION
NEGR1	Neuronal growth regulator 1	OBESITY	24.7	6.29	ND	UP
SEC16B	Protein transport protein Sec16B	OBESITY	116.0	5.71	ND	UP
ADIPOR1	Adiponectin receptor protein 1	OBESITY	42.6	6.53	Yes	Down
ADIPOR2	Adiponectin receptor protein 2	OBESITY	43.8	6.11	Yes	Down
TMEM18	Transmembrane protein 18	OBESITY	16.2	9.35	Yes	UP
INSIG2	Insulin-induced gene 2 protein	OBESITY	24.7	8.16	Yes	Down(ND)
ETV5	ETS translocation variant 5	OBESITY	57.8	5.43	Yes	Down
DGKG	Diacylglycerol kinase gamma	OBESITY	89.1	6.36	ND	ND
GNPDA2	Glucosamine-6-phosphate isomerase 2	OBESITY	31.0	6.45	Yes	Down
NCR3	Natural cytotoxicity triggering receptor 3	OBESITY	19.2	8.91	ND	ND
AIF1	Allograft inflammatory factor 1	OBESITY	16.7	5.97	Yes	Down
NAMPT	Nicotinamide phosphoribosyltransferase	OBESITY	55.5	6.69	Yes	Down(ND)
MTMR9	Myotubularin-related protein 9	OBESITY	63.4	5.98	Yes	Down(ND)
LPL	Lipoprotein lipase	OBESITY	53.1	8.37	Yes	Down
PTER	Phosphotriesterase-related protein	OBESITY	39.0	6.07	ND	ND
PFKP	6-phosphofructokinase	OBESITY	22.8	8.87	Yes	Down
MTCH2	Mitochondrial carrier homolog 2	OBESITY	33.3	8.25	Yes	UP
MAF	Transcription factor Maf	OBESITY	38.4	6.44	ND	UP
SH2B1	SH2B adapter protein 1	OBESITY	79.3	5.26	Yes	Down
MC4R	Melanocortin receptor 4	OBESITY	36.9	7.88	Yes	UP
KCTD15	BTB/POZ domain-containing protein KCTD15	OBESITY	31.9	7.05	Yes	Down
CTNNBL1	Beta-catenin-like protein 1	OBESITY	85.4	5.53	Yes	Down
NOTCH2	Neurogenic locus notch homolog protein 2	T2DM	132.1	4.65	Yes	=
THADA	Thyroid adenoma-associated protein	T2DM	219.6	5.71	Yes	Down
PPARG	Peroxisome proliferator-activated receptor gamma	T2DM	57.6	5.61	Yes	Down
ADAMTS9	A disintegrin & metalloproteinase with thrombospondin motifs 9	T2DM	216.4	8.13	Yes	=
IGF2BP2	Insulin-like growth factor 2 mRNA-binding protein 2	T2DM	66.1	8.48	Yes	Down
WFS1	Wolframin	T2DM	100.2	8.34	Yes	Down
CDKAL1	Threonylcarbamoyladenosine tRNA methylthiotransferase	T2DM	65.1	7.2	Yes	=
JAZF1	Juxtaposed with another zinc finger protein 1	T2DM	27.0	8.63	Yes	Down(ND)
SLC30A8	Zinc transporter 8	T2DM	40.7	6.11	ND	UP
CDKN2A	Cyclin-dependent kinase inhibitor 2A, isoform 4	T2DM	61.1	9.13	Yes	Down
CDKN2B	Cyclin-dependent kinase inhibitor 2B, isoform 4	T2DM	14.7	6.08	Yes	Down
CDC123	Cell division cycle protein 123 homolog	T2DM	32.1	4.63	Yes	Down
CAMK1D	Calcium/calmodulin-dependent protein kinase type 1D	T2DM	42.9	6.77	Yes	Down
HHEX	Hematopoietically-expressed homeobox protein HHEX	T2DM	23.9	7.10	ND	ND
TCF7L2	Transcription factor 7-like 2	T2DM	63.4	9.03	Yes	Down(ND)
KCNJ11	ATP-sensitive inward rectifier potassium channel 11	T2DM	43.5	8.15	ND	ND
TSPAN8	Tetraspanin-8	T2DM	26.4	5.48	Yes	=
LGR5	Leucine-rich repeat-containing G-protein coupled receptor 5	T2DM	99.9	6.12	Yes	Down(ND)
FTO	Alpha-ketoglutarate-dependent dioxygenase FTO	T2DM	58.2	5.10	Yes	Down
HNF1B	Protein regulator of cytokinesis 1	T2DM	61.3	7.39	ND	ND
PRC1	Glucokinase regulatory protein	T2DM	71.6	6.29	Yes	Down
GCKR	Transmembrane protein 195	T2DM	68.6	6.24	Yes	Down(ND)
TMEM195	Alkylglycerol monooxygenase	T2DM	51.5	7.75	Yes	UP
ZFAND6	AN1-type zinc finger protein 6	T2DM	22.5	6.87	Yes	Down(ND)
KCNJ6	G protein-activated inward rectifier potassium channel 2	T2DM	48.4	5.24	Yes	UP
CREB5	Cyclic AMP-responsive element-binding protein 5	T2DM	56.9	8.76	Yes	Down
PRDM6	Putative histone-lysine N-methyltransferase PRDM6	T2DM	64.4	7.93	Yes	=
GULP1	PTB domain-containing engulfment adapter protein 1	T2DM	34.4	8.04	Yes	UP
MTNR1B	Melatonin receptor type 1B	T2DM	40.1	9.12	ND	UP

Gene name, gene description, pI (isoelectric focusing point), the Molecular weight (Mw) and the mRNA expression of each studied gene were shown in this table. Other abbreviations and symbols are: ND (not detectable), Down (down-regulation), UP (Up-regulation) and = (equal mRNA expression of that gene was observed for adipocytes (control) and upon SPIONs treatment. The Mw was expressed in kDa. pI was resulted from whole amino acid sequence of each protein and derived from www.expasy.org.

T2D, and the prevalence of these diseases are increasing worldwide[2]. As SPIONs have several unique properties that maintain various medical applications such as drug delivery, transfection, and imaging[34], we studied the effect of SPIONs on the expression of the 22 and 29 genes-associated with obesity and T2D in human adipocytes respectively.

In order to mitigate any agglomeration of SPIONs and avoid possible shape related interference with our design[15], we used CES grafted SPIONs to stabilize particles and avoid agglomeration. The results of VSM and relaxometry analysis confirmed the superparamagnetic behavior along with success of coating. In fact, slight increase in magnetic saturation and relaxivity can be attributed to the increase of the weight and volume of magnetite nanoparticles after grafting with CES[35,36].

The reason why we have chosen these specific genes to study the effect of SPIONs is that these genes were found to be associated with
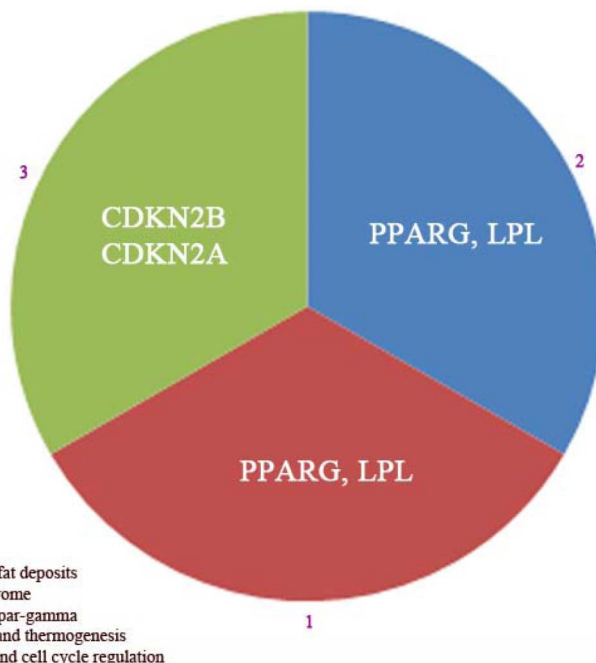
1. PID BioCarta: visceral fat deposits and the metabolic syndrome
2. PID BioCarta: role of ppar-gamma coactivators in obesity and thermogenesis
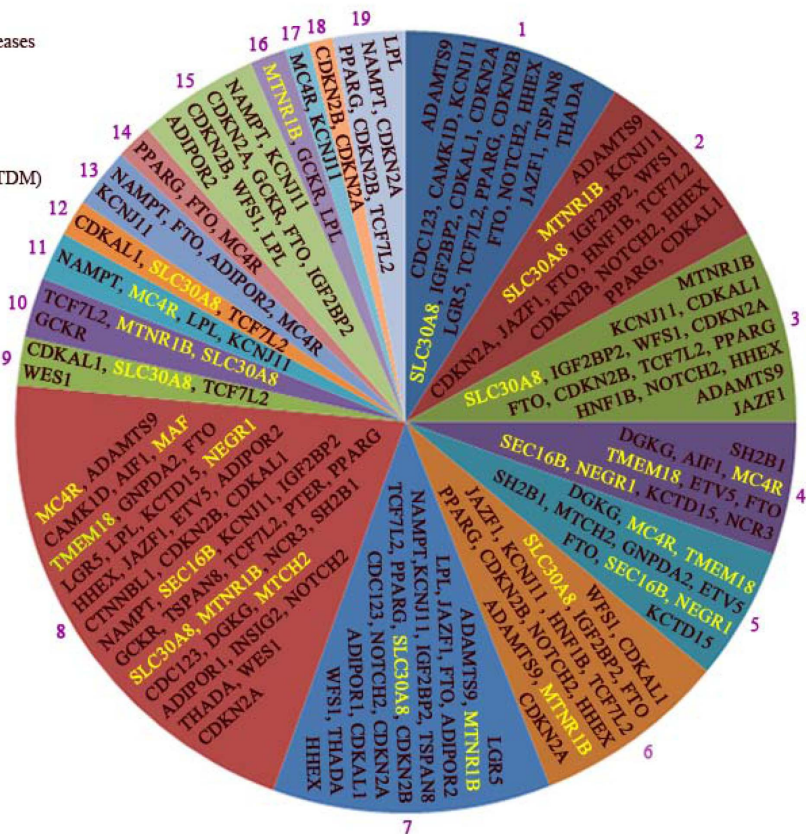3. PID BioCarta: cyclins and cell cycle regulation

Figure 9 │ Enriched functional pathways related to a combined set of the 22 and 29 genes found by GWAS as risk genes for obesity and type 2 diabetes (T2D) respectively. Only pathways with corrected p-values < 0.05 are presented. Pathway Interaction Database (PID) BioCarta was found significant. All three pathways were found by PID BioCarta database. The identified genes responsible for these three pathways are CDKN2A, CDKN2B, PPARγ and LPL (see also table 1).

1. GAD: Type II diabetes
2. KEGG DISEASE: Type II diabetes mellitus
3. KEGG DISEASE: Diabetes
4. GAD: Weight
5. GAD: Body mass index
6. KEGG DISEASE: Endocrine and metabolic diseases
7. GAD: Type II diabetes
8. GAD: METABOLIC
9. GAD: Type 2 diabetes and other traits
10. GAD: Fasting glucose-related traits
11. FunDO: Hyperinsulinism
12. GAD: Posttransplantation diabetes mellitus (PTDM)
13. FunDO: Polycystic ovary syndrome
14. GAD: Waist circumference
15. FunDO: Diabetes mellitus
16. GAD: Other metabolic traits
17. FunDO: Infantile spasms
18. FunDO: Actinic keratosis
19. GAD: Coronary Artery Disease

Figure 10 │ Enriched disorder pathways related to a combined set of the 22 and 29 genes found by GWAS as risk genes for obesity and type 2 diabetes (T2D) respectively. Only disorders with corrected p-values < 0.05 were included in the analysis. The complete list of gene abbreviations was shown in table 1. Kyoto Encyclopedia of Genes and Genomes (KEGG) pathway Genetic Association Database (GAD), and Functional disease ontology (FunDO) were found significant. The databases used in this combined set was, PIDcurated PID reactome, BioCyc, Reactome and Protein Analysis through Evolutionary Relationships (Panther) pathway databases and KEGG.

obesity and T2D in several and large genome-wide association studies (GWAS). Moreover, all these genes were also validated by single nucleotide polymorphisms (SNPs)[37].

For the functional pathway and disorder analysis in the current study, we include many databases. The increase of number of databases ensures the reduction of the chance for missing pathway(s). That was the reason why we applied multiple databases to detect the potential functional and disorder pathways link to the genes associated with obesity and T2D.

The pathway analysis ended to four functional pathways with ADIPOR1 and R2 as well as LPL as major genes in these pathways. These three genes play an important role in lipid metabolism and all function as anti T2D[31,38–41] and a reduction of these three genes contributes to the metabolic dysfunction and its associated disorders as consequences. However, all these three genes were down-regulated upon SPION treatment. This may mean that SPIONS has a disadvantage in this context. Interestingly, mRNA expression of 5 genes was found to be highly up-regulated upon SPIONs treatment of adipocytes, and the concrete function of some of them still under investigation. However, MTCH2 is involved in the depolarization of mitochondria[42]. Two scenarios is possible 1- upon SPIONs treatment, MTCH2 gene expresses very high, which in turn lead to the depolarization of mitochondria and as consequence the leaking of mitochondria membrane, and 2- if the first option is true; that means that SPIONs may enter the cell and may subsequently enter to the mitochondria.

The functions of GULP1 are to assist the phagocytosis of the apoptotic cells and also modulate the cholesterol transport[43]. Intriguingly, mRNA of GULP1 was highly expressed in SPIONs adipocytes as compared to control. In obese adipocytes, the efficiency of mitochondria function is reduced, long chain fatty acids will be accumulated within adipocytes. ATMs are meant to phagocyte the not functional components of the cells. It is already present reports that SPIONs produce ROS[44]. Thus, it may then logic to assume that SPIONs produce ROS, which, in turn, affect the mRNA expression of GULP1 that possibly contributes to the function of macrophages in the phagocytosis of apoptotic cells[43]. Thus, we are allowed to assume that this effect of SPIONs is a positive effect.

T2D-associated genes showed four functional pathways, which pointed to the cell cycle with the involvement of the following PPARγ, TCF7L2, CDKN2A, and CDKN2B genes. Notably, all these four genes from slightly to severely down-regulated in SPIONs adipocytes, indicating that cell cycle damage may contribute to the development of T2D and the use of SPIONs in biological application may affect the regulation of cell cycle[31]. Interestingly, we found that the most of genes associated with the risk for T2D were down-regulated after treatment of adipocytes with SPIONs and only one gene (i.e. SLC30A8) was up-regulated, which ensure the transport of accumulated Zinc to the intracellular vesicles[45]. Thus, SPIONs appeared to affect the expression of this gene. It must be noted that the function of some of these genes remained to be completed or to be under the investigations.

Surprisingly, after the combination of two clusters of genes, we observed only three pathways pointed to AT and cell cycle. This indicates that not only the role of adipocytes cannot be ignored in the development of obesity but also cell cycle may be a target of intervention for the therapy of these metabolic disorders. As it is already established, PPARγ and LPL are considered as anti-aging-related diseases such as T2D and atherosclerosis[32,46–48]. Based on this finding, we may cautiously assume that SPIONs may behave as pro-aging-linked disorders rather than anti-aging-related diseases.

Based on this study, we found that SPIONs play clearly a crucial role in the expression of the selected genes based on GWAS. The expression of some genes increases, while the expression of other genes decreased when we treated the adipocytes with SPIONs. Moreover, SPIONs may play dual roles (i.e. positive and negative).

Also, the application of SPIONs in human primary adipocytes as an established model for the study of energy metabolism provides us more knowledge about these types of NPs. We may cautiously conclude that SPIONs influence the gene expression of lipid and glucose metabolism. Thus, the effect of SPIONs must be extended to other cells in vitro and in particular in vivo. Also the interaction between SPIONs and adipocytes-secreted proteins must be investigated in future to gain more knowledge about the protein content of Corona (surface of SPIONs coated with proteins), which helps us to understand better the role of SPIONs in Nano- Biological application. We also find that the link between SPIONs, mitochondria, and adipocytes must not be ignored.

Methods

FeCl₂.4H₂O, FeCl₃.6H₂O, diethylene glycol, o-(2-aminoethyl)-o'-methylpolyethylene glycol (PEG-NH₂, MW = 750), and N,N-dimethylformamide (DMF) were purchased from Sigma-Aldrich, Germany. Carboxyethylsilanetriol (CES) was granted by Wacker-Chemie GmbH, Burghausen, Germany. Preadipocytes were purchased from LONZA (Belgium). All media and supplements for differentiation of the preadipocytes were provided by LONZA and PromoCell (Germany).

Synthesis of SPIONs. In order to obtain nanoparticles with a narrow size distribution, the polyol-method was employed[49]. Briefly, 5 mL of an aqueous solution of $FeCl_2.4H_2O$ (0.045 M) and $FeCl_{3.6H_2O}$ (0.0375 M) were added to 250 mL of diethyleneglycol. The mixture was heated to 170°C and maintained at this temperature for 15 min before addition of the base (i.e. solid NaOH (0.375 M). Subsequently, temperature was maintained at 170°C for a period of 1 h before cooling to 60°C. The synthesized SPIONs were collected with a neodymium magnet and washed with 100 mL of a HNO_3 (1 M) solution.

Grafting of SPIONs with Carboxyethylsilanetriol (CES). CES was grafted on the surfaces of SPIONs, as described elsewhere[49]. Briefly, 100 ml of nanoparticle solution (0.3 M iron) was added to 100 ml DMF and 45 ml of 0.15 M CES was slowly added before adding 25 ml water followed by 15 ml of NaOH solution (1 M) at room temperature and under homogenization (about 8000–24,000 rpm). The solution was heated to 100°C for 24 h under continuous stirring. The SPIONs were precipitated by addition of acetone/ether (50/50) mixture and collected with neodymium magnet. The precipitate was washed with acetone several times and finally dispersed in water. Excess of silane derivative and other chemicals were removed by dialysis using a dialysis bag (Spectrum Laboratories, Inc; MWCO = 10000) for 48 h in water.

Characterizations of SPIONs. Fourier transform infrared (FTIR) spectra were collected using a PerkinElmer Spectrum 100 spectrometer in the range of 4000–650 cm⁻¹, and each spectrum was obtained by averaging 32 interfere grams with a resolution of 4 cm⁻¹. Samples for FTIR analysis were prepared by lyophilizing SPION suspensions in water and a thin film of lyophilized SPIONs was placed on the attenuated total reflectance crystal for spectral recording.

The magnetization of the SPIONS in a variable magnetic field was measured using a vibrating-sample magnetometer (VSM) with a sensitivity of 10⁻³ emu and a maximum magnetic field of 10 kOe. The magnetic field was changed uniformly at a rate of 66 Oe/s.

The morphology and size of the particles was investigated using transmission electron microscopy (TEM),(ZEISS, EM-10C, Germany) operating at 100 kV. For sample preparation, a drop of the SPOIN suspension was placed on a copper grid and was dried under vacuum. Phase characterization was accomplished using the XRD (X-ray powder diffraction, Siemens, D5000, Germany) technique with Cu KR radiation, and the Scherrer method was used for particle size determination.

All these relexometric measurements were performed at room temperature. In the plot shown in this work, the magnetic field is expressed in terms of the proton Larmor frequency. The results are represented in terms of longitudinal relaxivities.

Cell culture. Human primary preadipocytes (Lonza) were culture to confluence in growth media provided by PromoCell in 5% CO2 at 37°C. When the cells reached confluence, the growth media were removed and replaced with preadipocyte differentiation FCS free media supplemented with (provided by promoCell) of 0.5 mM 3-isobutyl-1-methylxanthine, 400 ng/ml dexamethasone, 0.5 ug/ml bovine insulin, L-thyroxin 9 ng/ml, ciglitazone 3 ug/ml and d-biotin 8 ug/ml for 72 hours. After Three days, the differentiation media were removed and replaced with adipocyte nutrition medium containing 3% FCS, d-biotin 8 ug/ml, 0.5 ug/ml bovine insulin, and 400 ng/ml dexamethasone for a period of 16 days (terminal phase of differentiation). After maturation of adipocytes, the nutrition media were and the cells were washed 5 times with the differentiation FCS free media. After wash steps, the cells were incubated with the differentiation media with and without SPION for 30 h. Then the cells were washed with PBS for 5 times. Then the cells were lyzed and total RNA were extracted. The characterization of the cells was already established[2,50–52].

mRNA expression array. Total RNA was extracted from human primary adipocytes cultured in 6 wells (9 cm2). The quality and concentration of the RNA were

determined by Bioanalyser using the Agilent RNA 6000 Nano kit (Agilent, The Netherlands).

Total Prep RNA Amplification Kit was used to amplify and label the RNA. (Applied Biosystems, The Netherlands). Total RNA was used to make cDNA and the concentrations were determined in nanodrop. cRNA was used to Biotinylate applying RNA Amplification Kit (Ambion, Inc., Austin, TX) according to the manufacturer's instructions starting with 200 ng total RNA. Samples were purified using the RNeasy kit (Qiagen, Valencia, CA). Hybridization to the Sentrix HumanRef-12 Expression BeadChip array (Illumina, San Diego, CA, USA), washing, and scanning were performed according to the Illumina BeadStation 500 manual (revision C). One BeadChip with twelve arrays were used. Slide was scanned immediately.

After the scanning, the following steps were performed: 1- quality check, 2- background correction, and utile normalization of the data using Beadstudio Expression module v 3.2.7. and 3- Statistics and the generation of gene lists using Genespring GX 7.3.1 (Agilent). P-values were corrected for multiple testing using Benjamini and Hochberg False Discovery Rates.

Functional and disorder pathway analysis. KOBAS version 2.0 combined with hypergeometric test and Benjamini-Hochberg FDR correction were performed to screen the enriched pathways and disorders, which obesity- and T2D-associated genes may have a role[53].

1. Xu, H. *et al*. Chronic inflammation in fat plays a crucial role in the development of obesity-related insulin resistance. *J Clin Invest* **112**, 1821–1830 (2003).
2. Meijer, K. *et al*. Human primary adipocytes exhibit immune cell function: adipocytes prime inflammation independent of macrophages. *PLoS One* **6**, e17154 (2011).
3. Calabro, P. *et al*. Adipose tissue-mediated inflammation: the missing link between obesity and cardiovascular disease? *Intern Emerg Med* **4**, 25–34 (2009).
4. Kahn, B. B. & Flier, J. S. Obesity and insulin resistance. *J Clin Invest* **106**, 473–481 (2000).
5. Nadler, S. T. *et al*. The expression of adipogenic genes is decreased in obesity and diabetes mellitus. *Proc Natl Acad Sci U S A* **97**, 11371–11376 (2000).
6. Scherer, P. E. Adipose tissue: from lipid storage compartment to endocrine organ. *Diabetes* **55**, 1537–1545 (2006).
7. Weisberg, S. P. *et al*. Obesity is associated with macrophage accumulation in adipose tissue. *J Clin Invest* **112**, 1796–1808 (2003).
8. Zeyda, M. *et al*. Human adipose tissue macrophages are of an anti-inflammatory phenotype but capable of excessive pro-inflammatory mediator production. *Int J Obes (Lond)* **31**, 1420–1428 (2007).
9. Bell, C. G., Walley, A. J. & Froguel, P. The genetics of human obesity. *Nat Rev Genet* **6**, 221–234 (2005).
10. O'Rahilly, S., Barroso, I. & Wareham, N. J. Genetic factors in type 2 diabetes: the end of the beginning? *Science* **307**, 370–373 (2005).
11. Takamura, T. *et al*. Obesity upregulates genes involved in oxidative phosphorylation in livers of diabetic patients. *Obesity (Silver Spring)* **16**, 2601–2609 (2008).
12. Bradfield, J. P. *et al*. A genome-wide association meta-analysis identifies new childhood obesity loci. *Nat Genet* **44**, 526–531 (2012).
13. Choi, J. K. & Kim, S. C. Environmental effects on gene expression phenotype have regional biases in the human genome. *Genetics* **175**, 1607–1613 (2007).
14. Mahmoudi, M., Azadmanesh, K., Shokrgozar, M. A., Journeay, W. S. & Laurent, S. Effect of nanoparticles on the cell life cycle. *Chem Rev* **111**, 3407–3432 (2011).
15. Sharifi, S. *et al*. Toxicity of nanomaterials. *Chem Soc Rev* **41**, 2323–2343 (2012).
16. Monopoli, M. P. *et al*. Physical-chemical aspects of protein corona: relevance to in vitro and in vivo biological impacts of nanoparticles. *J Am Chem Soc* **133**, 2525–2534 (2011).
17. Walczyk, D., Bombelli, F. B., Monopoli, M. P., Lynch, I. & Dawson, K. A. What the cell "sees" in bionanoscience. *J Am Chem Soc* **132**, 5761–5768 (2010).
18. Hauck, T. S., Ghazani, A. A. & Chan, W. C. Assessing the effect of surface chemistry on gold nanorod uptake, toxicity, and gene expression in mammalian cells. *Small* **4**, 153–159 (2008).
19. Rahman, M. F. *et al*. Expression of genes related to oxidative stress in the mouse brain after exposure to silver-25 nanoparticles. *Toxicol Lett* **187**, 15–21 (2009).
20. Shimizu, M. *et al*. Maternal exposure to nanoparticulate titanium dioxide during the prenatal period alters gene expression related to brain development in the mouse. *Part Fibre Toxicol* **6**, 20 (2009).
21. Bulte, J. W., Duncan, I. D. & Frank, J. A. In vivo magnetic resonance tracking of magnetically labeled cells after transplantation. *J Cereb Blood Flow Metab* **22**, 899–907 (2002).
22. Bulte, J. W. *et al*. Magnetodendrimers allow endosomal magnetic labeling and in vivo tracking of stem cells. *Nat Biotechnol* **19**, 1141–1147 (2001).
23. Lewin, M. *et al*. Tat peptide-derivatized magnetic nanoparticles allow in vivo tracking and recovery of progenitor cells. *Nat Biotechnol* **18**, 410–414 (2000).
24. Dave, S. R. & Gao, X. Monodisperse magnetic nanoparticles for biodetection, imaging, and drug delivery : a versatile and evolving technology. *Wiley Interdiscip Rev Nanomed Nanobiotechnol* **1**, 583–609 (2009).
25. Mahmoudi, M., Simchi, A., Imani, M. & Häfeli, U. O. Superparamagnetic Iron Oxide Nanoparticles with Rigid Cross-linked Polyethylene Glycol Fumarate Coating for Application in Imaging and Drug Delivery. *The Journal of Physical Chemistry C* **113**, 8124–8131 (2009).
26. Unfried, K. *et al*. Cellular responses to nanoparticles: Target structures and mechanisms. *Nanotoxicology* **1**, 52–71 (2007).
27. Moller, P. *et al*. Role of oxidative damage in toxicity of particulates. *Free Radic Res* **44**, 1–46 (2010).
28. Nel, A., Xia, T., Madler, L. & Li, N. Toxic potential of materials at the nanolevel. *Science* **311**, 622–627 (2006).
29. Chrysohoou, C. *et al*. The implication of obesity on total antioxidant capacity in apparently healthy men and women: the ATTICA study. *Nutr Metab Cardiovasc Dis* **17**, 590–597 (2007).
30. Esposito, K. *et al*. Oxidative stress in the metabolic syndrome. *J Endocrinol Invest* **29**, 791–795 (2006).
31. Quelle, D. E., Zindy, F., Ashmun, R. A. & Sherr, C. J. Alternative reading frames of the INK4a tumor suppressor gene encode two unrelated proteins capable of inducing cell cycle arrest. *Cell* **83**, 993–1000 (1995).
32. Enerback, S., Ohlsson, B. G., Samuelsson, L. & Bjursell, G. Characterization of the human lipoprotein lipase (LPL) promoter: evidence of two cis-regulatory regions, LP-alpha and LP-beta, of importance for the differentiation-linked induction of the LPL gene during adipogenesis. *Mol Cell Biol* **12**, 4622–4633 (1992).
33. Ristow, M., Muller-Wieland, D., Pfeiffer, A., Krone, W. & Kahn, C. R. Obesity associated with a mutation in a genetic regulator of adipocyte differentiation. *N Engl J Med* **339**, 953–959 (1998).
34. Mahmoudi, M., Sant, S., Wang, B., Laurent, S. & Sen, T. Superparamagnetic iron oxide nanoparticles (SPIONs): development, surface modification and applications in chemotherapy. *Adv Drug Deliv Rev* **63**, 24–46 (2011).
35. Mahmoudi, M., Simchi, A., Imani, M., Milani, A. S. & Stroeve, P. Optimal Design and Characterization of Superparamagnetic Iron Oxide Nanoparticles Coated with Polyvinyl Alcohol for Targeted Delivery and Imaging. *J Phys Chem B* **112**, 14470–14481 (2008).
36. LaConte, L. E. *et al*. Coating thickness of magnetic iron oxide nanoparticles affects R2 relaxivity. *J Magn Reson Imaging* **26**, 1634–1641 (2007).
37. Tsai, F.-J. *et al*. A Genome-Wide Association Study Identifies Susceptibility Variants for Type 2 Diabetes in Han Chinese. *PLoS Genet* **6**, e1000847 (2010).
38. Yamauchi, T. *et al*. Cloning of adiponectin receptors that mediate antidiabetic metabolic effects. *Nature* **423**, 762–769 (2003).
39. Kotronen, A. *et al*. Genetic variation in the ADIPOR2 gene is associated with liver fat content and its surrogate markers in three independent cohorts. *Eur J Endocrinol* **160**, 593–602 (2009).
40. Benlian, P. *et al*. Premature atherosclerosis in patients with familial chylomicronemia caused by mutations in the lipoprotein lipase gene. *New Engl J Med* **335**, 848–854 (1996).
41. Chan, L. Y. *et al*. Genotype-phenotype studies of six novel LPL mutations in Chinese patients with hypertriglyceridemia. *Hum Mutat* **20**, 232–233 (2002).
42. Yerushalmi, G. M., Leibowitz-Amit, R., Shaharabany, M. & Tsarfaty, I. Met-HGF/SF signal transduction induces mimp, a novel mitochondrial carrier homologue, which leads to mitochondrial depolarization. *Neoplasia* **4**, 510–522 (2002).
43. Smits, E., Van Criekinge, W., Plaetinck, G. & Bogaert, T. The human homologue of Caenorhabditis elegans CED-6 specifically promotes phagocytosis of apoptotic cells. *Curr Biol* **9**, 1351–1354 (1999).
44. Singh, N., Jenkins, G. J., Asadi, R. & Doak, S. H. Potential toxicity of superparamagnetic iron oxide nanoparticles (SPION). *Nano Rev* **1** (2010).
45. Chimienti, F. *et al*. In vivo expression and functional characterization of the zinc transporter ZnT8 in glucose-induced insulin secretion. *J Cell Sci* **119**, 4199–4206 (2006).
46. Ristow, M., Muller-Wieland, D., Pfeiffer, A., Krone, W. & Kahn, C. R. Obesity associated with a mutation in a genetic regulator of adipocyte differentiation. *New Engl J Med* **339**, 953–959 (1998).
47. Mukherjee, R., Jow, L., Croston, G. E. & Paterniti, J. R., Jr. Identification, characterization, and tissue distribution of human peroxisome proliferator-activated receptor (PPAR) isoforms PPARgamma2 versus PPARgamma1 and activation with retinoid X receptor agonists and antagonists. *J Biol Chem* **272**, 8071–8076 (1997).
48. Yin, Y. Z. *et al*. 3-Phosphoinositide-dependent protein kinase-1 activates the peroxisome proliferator-activated receptor-gamma and promotes adipocyte differentiation. *Mol Endocrinol* **20**, 268–278 (2006).
49. Forge, D. *et al*. Optimization of the Synthesis of Superparamagnetic Contrast Agents by the Design of Experiments Method. *The Journal of Physical Chemistry C* **112**, 19178–19185 (2008).
50. Xu, Z., Liu, Q. & Finch, J. A. Silanation and stability of 3-aminopropyl triethoxy silane on nanosized superparamagnetic particles: I. Direct silanation. *Applied Surface Science* **120**, 269–278 (1997).
51. Dashty, M. *et al*. Characterization of coagulation factor synthesis in nine human primary cell types. *Sci Rep* **2**, 787 (2012).
52. Queiroz, K. C. *et al*. Human plasma very low density lipoprotein carries Indian hedgehog. *J Proteome Res* **9**, 6052–6059 (2010).
53. Xie, C. *et al*. KOBAS 2.0: a web server for annotation and identification of enriched pathways and diseases. *Nucleic Acids Res* **39**, W316–322 (2011).

Author contributions

experiments. All authors; S.S., S.D., M.M.M., B.B., B.S., A.K., A.R., S.L., M.P.P., F.R. participated in the analyzing data and contributed to the editing of the paper.

Additional information